Search for Periodic Time Variations of the Solar ⁸B Neutrino Flux between 1996 and 2018 in Super-Kamiokande

K. Abe, 1.46 C. Bronner, ¹ Y. Hayato, ^{1.46} K. Hiraide, ^{1.46} K. Hosokawa, ¹ K. Ieki, ^{1.46} M. Ikeda, ^{1.46} J. Kameda, ^{1.46} Y. Kanemura, ¹ R. Kaneshima, ¹ Y. Kashiwagi, ¹ Y. Kataoka, ^{1.46} S. Miki, ¹ S. Mine, ^{1.6} M. Miura, ^{1.46} S. Moriyama, ^{1.46} Y. Nakano, ¹ M. Nakahata, ^{1.46} S. Nakayama, ^{1.46} Y. Noguchi, ¹ K. Sato, ¹ H. Sekiya, ^{1.46} H. Shiba, ¹ K. Shimizu, ¹ M. Shiozawa, ^{1.46} Y. Sonoda, ¹ Y. Suzuki, ¹ A. Takeda, ^{1.46} Y. Takemoto, ^{1.46} H. Tanaka, ^{1.46} T. Yano, ¹ S. Han, ² T. Kajita, ^{2.46,22} K. Okumura, ^{2.46} E. Keams, ^{4.46} J. L. Raaf, ⁴ L. Wan, ⁴ T. Wester, ⁴ J. Bian, ⁶ N. J. Griskevich, ⁶ S. Locke, ⁶ M. B. Smy, ^{4.46} H. W. Sobel, ^{6.46} V. Takhistov, ^{6.24} A. Yankelevich, ⁶ J. Hill, ⁷ S. H. Lee, ⁸ D. H. Moon, ⁸ R. G. Park, ⁸ M. C. Jang, ⁸ B. Bodur, ⁹ K. Scholberg, ^{9.46} C. W. Walter, ^{9.46} A. Beauchêne, ¹⁰ O. Drapier, ¹⁰ A. Giampaolo, ¹⁰ Th. A. Mueller, ¹⁰ A. D. Santos, ¹⁰ P. Paganini, ¹⁰ B. Quilain, ¹⁰ T. Nakamura, ¹¹ J. S. Jang, ¹² L. N. Machado, ¹³ J. G. Learned, ¹⁴ K. Choi, ¹⁵ N. Iovine, ¹⁵ S. Cao, ¹⁶ L. H. V. Anthony, ¹⁷ D. Martin, ¹⁷ N. W. Prouse, ¹⁷ M. Scott, ¹⁷ A. A. Sztuc, ¹⁷ Y. Uchida, ¹⁷ V. Berardi, ¹⁸ M. G. Catanesi, ¹⁸ E. Radicioni, ¹⁸ N. F. Calabria, ¹⁹ A. Langella, ¹⁹ G. De Rosa, ¹⁹ G. Collazuol, ²⁰ F. Iacob, ²⁰ M. Mattiazzi, ²⁰ L. Ludovici, ²¹ M. Hasegawa, ²⁴ T. Ishida, ²⁴ T. Kobayashi, ²⁴ M. Jakkapu, ²⁴ T. Matsubara, ²⁴ T. Nakadaira, ²⁴ K. Nakamura, ^{24,46} Y. Oyama, ²⁴ K. Sakashita, ²⁴ T. Sekiguchi, ²⁴ T. Tsukamoto, ²⁴ N. Bhuiyan, ²⁵ G. T. Burton, ²⁵ F. Di Lodovico, ²⁵ J. Gao, ²⁵ A. Goldsack, ²⁵ T. Katori, ²⁵ J. Migenda, ²⁵ Z. Xie, ²⁵ R. M. Ramsden, ²⁵ S. Zsoldos, ^{25,46} A. T. Suzuki, ²⁶ Y. Takagi, ²⁶ H. Zhong, ²⁶ Y. Takagi, ²⁶ H. Zhong, ³⁰ Y. Jakauchi, ^{26,46} J. Feng, ²⁷ L. Feng, ²⁷ J. R. Hu, ²⁷ Z. Hu, ²⁷ T. Kikawa, ²⁷ M. Mori, ²⁷ M. Kawaue, ²⁷ T. Nakaya, ^{27,46} K. Nakanishi, ³

(Super-Kamiokande Collaboration)

¹Kamioka Observatory, Institute for Cosmic Ray Research, University of Tokyo, Kamioka, Gifu 506-1205, Japan

²Research Center for Cosmic Neutrinos, Institute for Cosmic Ray Research, University of Tokyo, Kashiwa, Chiba 277-8582, Japan ³Department of Theoretical Physics, University Autonoma Madrid, 28049 Madrid, Spain ⁴Department of Physics, Boston University, Boston, Massachusetts 02215, USA ⁵Department of Physics, British Columbia Institute of Technology, Burnaby, British Columbia V5G 3H2, Canada ⁶Department of Physics and Astronomy, University of California, Irvine, Irvine, California 92697-4575, USA Department of Physics, California State University, Dominguez Hills, Carson, California 90747, USA 8 Institute for Universe and Elementary Particles, Chonnam National University, Gwangju 61186, Korea ⁹Department of Physics, Duke University, Durham, North Carolina 27708, USA ¹⁰Ecole Polytechnique, IN2P3-CNRS, Laboratoire Leprince-Ringuet, F-91120 Palaiseau, France ¹¹Department of Physics, Gifu University, Gifu, Gifu 501-1193, Japan ¹²GIST College, Gwangju Institute of Science and Technology, Gwangju 500-712, Korea ¹³School of Physics and Astronomy, University of Glasgow, Glasgow, Scotland G12 8QQ, United Kingdom ⁴Department of Physics and Astronomy, University of Hawaii, Honolulu, Hawaii 96822, USA ¹⁵Center for Underground Physics, Institute for Basic Science (IBS), Daejeon, 34126, Korea ¹⁶Institute For Interdisciplinary Research in Science and Education, ICISE, Quy Nhon 55121, Vietnam

```
<sup>17</sup>Department of Physics, Imperial College London, London SW7 2AZ, United Kingdom
   <sup>18</sup>Dipartimento Interuniversitario di Fisica, INFN Sezione di Bari and Università e Politecnico di Bari, I-70125 Bari, Italy
                 <sup>19</sup>Dipartimento di Fisica, INFN Sezione di Napoli and Università di Napoli, I-80126 Napoli, Italy
               <sup>20</sup>Dipartimento di Fisica, INFN Sezione di Padova and Università di Padova, I-35131 Padova, Italy
                      <sup>21</sup>INFN Sezione di Roma and Università di Roma "La Sapienza", I-00185 Roma, Italy
          <sup>22</sup>ILANCE, CNRS - University of Tokyo International Research Laboratory, Kashiwa, Chiba 277-8582, Japan
                        <sup>23</sup>Department of Physics, Keio University, Yokohama, Kanagawa, 223-8522, Japan
                   <sup>24</sup>High Energy Accelerator Research Organization (KEK), Tsukuba, Ibaraki 305-0801, Japan
                       Department of Physics, King's College London, London WC2R 2LS, United Kingdom
                             <sup>26</sup>Department of Physics, Kobe University, Kobe, Hyogo 657-8501, Japan
                             <sup>27</sup>Department of Physics, Kyoto University, Kyoto, Kyoto 606-8502, Japan
                      <sup>28</sup>Department of Physics, University of Liverpool, Liverpool L69 7ZE, United Kingdom
                    <sup>29</sup>Department of Physics, Miyagi University of Education, Sendai, Miyagi 980-0845, Japan
             <sup>30</sup>Institute for Space-Earth Environmental Research, Nagoya University, Nagoya, Aichi 464-8602, Japan
<sup>31</sup>Kobayashi-Maskawa Institute for the Origin of Particles and the Universe, Nagoya University, Nagoya, Aichi 464-8602, Japan
                                  <sup>2</sup>National Centre For Nuclear Research, 02-093 Warsaw, Poland
       <sup>33</sup>Department of Physics and Astronomy, State University of New York at Stony Brook, New York 11794-3800, USA
                        <sup>34</sup>Department of Physics, Okayama University, Okayama, Okayama 700-8530, Japan
         <sup>35</sup>Media Communication Center, Osaka Electro-Communication University, Neyagawa, Osaka 572-8530, Japan
                          <sup>36</sup>Department of Physics, Oxford University, Oxford OX1 3PU, United Kingdom
                         <sup>37</sup>Rutherford Appleton Laboratory, Harwell, Oxford OX11 0QX, United Kingdom
                             <sup>38</sup>Department of Physics, Seoul National University, Seoul 151-742, Korea
               <sup>39</sup>Department of Physics and Astronomy, University of Sheffield, Sheffield S3 7RH, United Kingdom
        <sup>40</sup>Department of Informatics in Social Welfare, Shizuoka University of Welfare, Yaizu, Shizuoka 425-8611, Japan
<sup>41</sup>STFC, Rutherford Appleton Laboratory, Harwell Oxford, and Daresbury Laboratory, Warrington OX11 0QX, United Kingdom
                            <sup>42</sup>Department of Physics, Sungkyunkwan University, Suwon 440-746, Korea
                <sup>43</sup>Department of Physics, Faculty of Science, Tohoku University, Sendai, Miyagi 980-8578, Japan
                         <sup>4</sup>Department of Physics, Tokai University, Hiratsuka, Kanagawa 259-1292, Japan
                          <sup>45</sup>Department of Physics, University of Tokyo, Bunkyo, Tokyo 113-0033, Japan
<sup>46</sup>Kavli Institute for the Physics and Mathematics of the Universe (WPI), The University of Tokyo Institutes for Advanced Study,
                                       University of Tokyo, Kashiwa, Chiba 277-8583, Japan
                     <sup>47</sup>Department of Physics, Tokyo Institute of Technology, Meguro, Tokyo 152-8551, Japan
    <sup>48</sup>Department of Physics, Faculty of Science and Technology, Tokyo University of Science, Noda, Chiba 278-8510, Japan
                         <sup>49</sup>TRIUMF, 4004 Wesbrook Mall, Vancouver, British Columbia V6T2A3, Canada
                         <sup>50</sup>Department of Engineering Physics, Tsinghua University, Beijing 100084, China
                                <sup>51</sup>Faculty of Physics, University of Warsaw, Warsaw 02-093, Poland
                       <sup>52</sup>Department of Physics, University of Warwick, Coventry CV4 7AL, United Kingdom
                            Department of Physics, University of Winnipeg, Manitoba R3J 3L8, Canada
                <sup>54</sup>Department of Physics, Yokohama National University, Yokohama, Kanagawa 240-8501, Japan
```

(Received 8 November 2023; revised 20 February 2024; accepted 12 April 2024; published 14 June 2024)

We report a search for time variations of the solar 8B neutrino flux using 5804 live days of Super-Kamiokande data collected between May 31, 1996, and May 30, 2018. Super-Kamiokande measured the precise time of each solar neutrino interaction over 22 calendar years to search for solar neutrino flux modulations with unprecedented precision. Periodic modulations are searched for in a dataset comprising five-day interval solar neutrino flux measurements with a maximum likelihood method. We also applied the Lomb-Scargle method to this dataset to compare it with previous reports. The only significant modulation found is due to the elliptic orbit of the Earth around the Sun. The observed modulation is consistent with astronomical data: we measured an eccentricity of $(1.53 \pm 0.35)\%$, and a perihelion shift of (-1.5 ± 13.5) days.

DOI: 10.1103/PhysRevLett.132.241803

Published by the American Physical Society under the terms of the Creative Commons Attribution 4.0 International license. Further distribution of this work must maintain attribution to the author(s) and the published article's title, journal citation, and DOI. Funded by SCOAP³. Introduction.—Solar neutrino observations are critical for investigating stars and learning about neutrino physics. The observation of solar neutrinos proves that nuclear fusion powers the Sun. The solar neutrinos carry real-time information about the solar core, while photons take a long

time to reach the photosphere. Solar dynamics may cause fluctuations in the solar neutrino flux. The experimental confirmation of neutrino oscillations with solar neutrinos solved the long-standing solar neutrino problem (e.g., the observed average flux of ⁸B neutrinos is as expected [1–5]), as well as measured oscillation parameters [6–8].

In addition, instantaneous changes in the solar magnetic field could modify the neutrino flux if the neutrino has a magnetic moment. If neutrinos are Dirac particles with a nonvanishing magnetic moment, the magnetic field will rotate the neutrino spin orientation. This process is known as resonant spin flavor precession (RSFP) [9–11]. The process can occur on the inner tachocline, where a strong magnetic field is formed [12]. Because the spin-flipped right-handed neutrinos are sterile, RSFP would reduce the observed solar neutrino fluxes. If neutrinos are Majorana particles with a flavor-changing magnetic moment, the solar magnetic field could convert a ν_e into a $\bar{\nu}_{\mu}$ or a $\bar{\nu}_{\tau}$, reducing the observed solar neutrino due to the suppressed elastic scattering cross sections. Therefore, any time variation in the magnetic fields in the Sun could result in modulations in the observed solar neutrino fluxes. The rotation profile of the interior of the Sun is known for $R > 0.2 R_{\rm sun}$ where $R_{\rm sun}$ is the solar radius. The radiative zone of the Sun in $0.3 R_{\rm sun} < R < 0.7 R_{\rm sun}$ is assumed to be a solid body rotating at a constant rate [13]. The rotation profile suggests the existence of a magnetic field in the radiative zone. The observations of splitting frequencies of the solar neutrino flux modulation can be used to infer the magnetic field. Observing a periodic modulation in the solar neutrino flux would be a significant breakthrough in understanding neutrinos' magnetic properties and the dynamics of the Sun's inside. We investigate the periodicity of solar neutrino fluxes using the observed Super-Kamiokande (SK) solar neutrino data.

Super-Kamiokande is a water Cherenkov detector in Kamioka, Japan, with a total mass of 50 kt [14]. The solar neutrino data in this analysis were obtained from May 31, 1996, to May 30, 2018, totaling 5803 days of detector live time. Table I summarizes the periods of data samples, live time, energy range, and overall systematic uncertainties of the solar neutrino flux measurements. While the elastic scattering rate of solar ⁸B (99.8%) and hep (0.2%) neutrinos in the SK water is expected to be about 300 per day,

most resulting recoil electrons are too low in energy to be observable. Accounting for energy threshold, detector efficiencies, and neutrino oscillations, about 20 solar neutrino interactions per day are observed, while about 45 solar neutrino interactions per day are expected. With this high rate, we search for periodic modulations with periods as short as five days. A comprehensive description of the SK detector can be found in Refs. [1–4].

Solar neutrino events produce recoil electrons through neutrino-electron scattering, preferentially aligned with the Sun's direction. We calculate the angle $\cos \theta_{\text{sun}}$ for each elastic scattering event between the reconstructed Cherenkov ring direction and the Sun's direction. The data sample is divided into $N_{\rm bin}=21$ energy bins: 18 energy bins between 5 and 14 MeV ($\Delta E = 0.5$ MeV), two energy bins between 14 and 16 MeV ($\Delta E = 1$ MeV), and one bin between 16 and 20 MeV. We perform a maximum likelihood fit to the $\cos \theta_{\text{sun}}$ distribution in each energy bin i to the number of solar neutrino interactions S and the numbers of radioactive background events B_i [4]. Each of the n_i events in energy bin i is assigned a signal factor s_{ik} and a background factor b_{ik} depending on $\cos \theta_{sun}$: with the probability density function p for signal (u for background) these factors are $s_{ik} = p(\cos \theta_k, E_i)$ and $b_{ik} = u(\cos\theta_k, E_i).$

$$\mathcal{L} = e^{-(\sum_i B_i + S)} \prod_{i=1}^{N_{\mathrm{bin}}} \prod_{\kappa=1}^{n_i} \left(B_i b_{i\kappa} + S \frac{\mathrm{MC}_i}{\sum_j \mathrm{MC}_j} s_{i\kappa} \right).$$

The \mathcal{L} is maximized by optimizing the signal S and the 21 backgrounds B_i . MC_i is the number of events expected in energy bin i using the flux and spectrum of 8B and hep neutrinos assuming no neutrino oscillation. The systematic uncertainties of the neutrino flux measurements consist of energy-correlated and uncorrelated errors. The total uncertainty of the flux is obtained by combining both errors. Table I lists the total systematic uncertainty for each SK period. References [1–4] describe the systematic uncertainties for the solar neutrino flux measurements. The Sudbury Neutrino Observatory (SNO) measured all active flavors of the solar 8B neutrino flux and found $(5.25 \pm 0.2) \times 10^6$ cm⁻² s⁻¹ [15]. This analysis used this value as a reference for solar neutrino flux.

TABLE I. Super-Kamiokande (SK) operation period, live time, energy range, total flux, statistical, and systematic uncertainties of the total flux. The neutrino flux is measured from elastic scattering recoil electrons. For SK-III, 3.99–4.49 MeV is not used; for SK-IV, 3.49–4.49 MeV is not used in the data.

SK Phase	Start date-End date	Live days	Energy range (MeV)	Flux (ϕ_{ν}) + (stat) + (sys) [10 ⁶ cm ⁻² s ⁻¹]
SK-I	1996-05-31-2001-07-15	1495.7	4.49-19.5	$2.35 \pm 0.02 \pm 0.08$
SK-II	2002-12-10-2005-10-06	791.9	6.49-19.5	$2.38 \pm 0.05^{+0.16}_{-0.15}$
SK-III	2006-05-23-2008-08-17	548.5	4.49-19.5	$2.32 \pm 0.04 \pm 0.05$
SK-IV	2008-09-15-2018-05-30	2967.7	4.49–19.5	$2.31 \pm 0.014 \pm 0.040$

Search for periodic modulation.—To search for periodic variations of the solar neutrino flux, five-day intervals are defined: 358 for SK-I [16], 175 for SK-II, 141 for SK-III, and 669 for SK-IV (total 1343 intervals). The solar neutrino interactions (and uncertainties) are obtained in each interval with the same extended unbinned maximum likelihood method mentioned in the previous section. The flux of ⁸B solar neutrinos is calculated from the observed event rate without assuming the effect of neutrino flavor oscillation. Additionally, no corrections are applied to the flux result for the distance between the Sun and the Earth, which varies annually around 1 A.U. The detector operation time is considered by choosing the weighted mean time as the

effective time of the five-day interval. Figure 1 shows five-day and 45-day (average of nine five-day interval data for each bin) intervals of solar neutrino fluxes for all SK phases without corrections for the distance between the Sun and the Earth, which varies annually around 1 A.U. We provide the data for five-day interval fluxes and the measurement time in the Supplemental Material [17]. The statistical uncertainty of the five-day interval flux is an asymmetric Gaussian form of the extracted likelihoods. The upper and lower uncertainties of the five-day data point are the displacements from the measured flux at which the profiled likelihood decreases by a factor of $e^{-1/2}$. The data used for the modulation likelihood is corrected by multiplying the

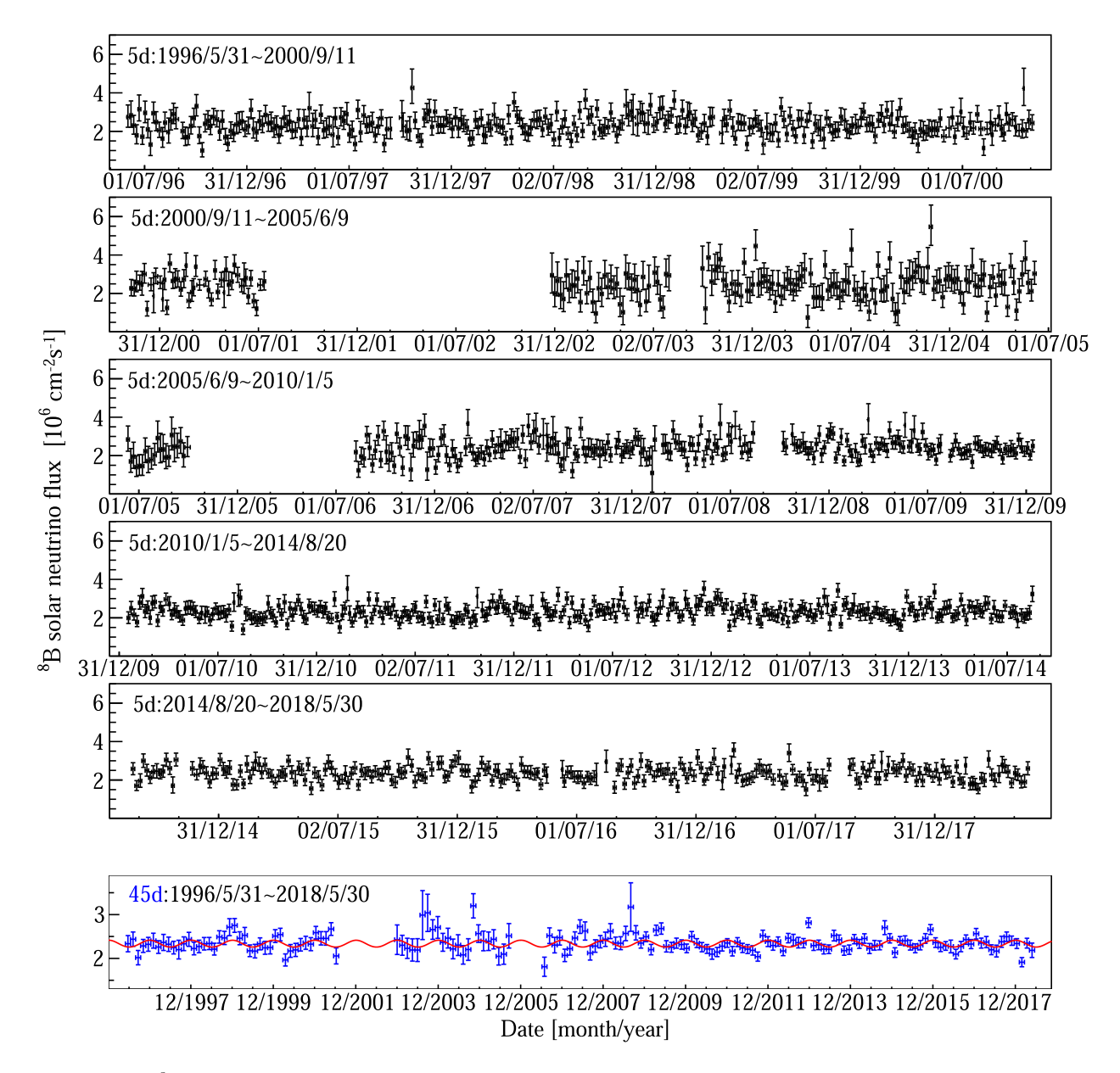


FIG. 1. Measured 8B solar neutrino fluxes for five-day (top five panels, black data points) and 45-day (bottom panel, blue data points) intervals without $1/R^2$ correction. The five-day (45-day) plot errors are asymmetric (symmetric) errors of the average fluxes. The solid-red curve in the 45-day plot is the expected sinusoidal solar neutrino flux based on the Earth's elliptical orbit.

squared distance between the Sun and the Earth. The predicted flux in the time bin is obtained by

$$g_r(\omega; A, B) = g_0 + \frac{1}{t_{r,f} - t_{r,i}} \int_{t_{r,i}}^{t_{r,f}} dt (A\cos\omega t + B\sin\omega t),$$

where the frequency (ω) is scanned with a step of $2 \times 10^{-6} \, \mathrm{days^{-1}}$ and amplitudes $(A \, \mathrm{and} \, B)$ are free parameters, $t_{r,i}$ is the initial and $t_{r,f}$ is the final time of the rth time interval. g_0 is the average of all data points. A log-likelihood is defined as

$$-\log \mathcal{L} = \min_{A,B} \left[\frac{1}{2} \sum_{r} \left(\frac{D_r - g_r(\omega; A, B)}{\sigma_r} \right)^2 \right],$$

where D_r is the data point at r, and σ_r is the asymmetric statistical uncertainty $\sigma_{+,r}$ ($\sigma_{-,r}$) for $D_r < g_r$ ($D_r > g_r$). The likelihood of the null hypothesis (\mathcal{L}_0) is tested by setting the A = B = 0. The power of the likelihood is defined as $P_L = -\log(\mathcal{L}_0/\mathcal{L})$. It is assumed that the average of the second term of the g_r equation never deviated from zero for any frequencies. Ten thousand Monte Carlo (MC) samples are generated assuming the null hypothesis to examine a broad range of modulation frequencies. Each MC sample consists of asymmetric Gaussian variations with mean g_0 and errors given by the upper and lower statistical uncertainties in each interval. Then, the power for each MC set is calculated at all tested frequencies, and the maximum power for each MC set is selected. The area of the maximum power distribution less than the corresponding power gives the (1 - p) value.

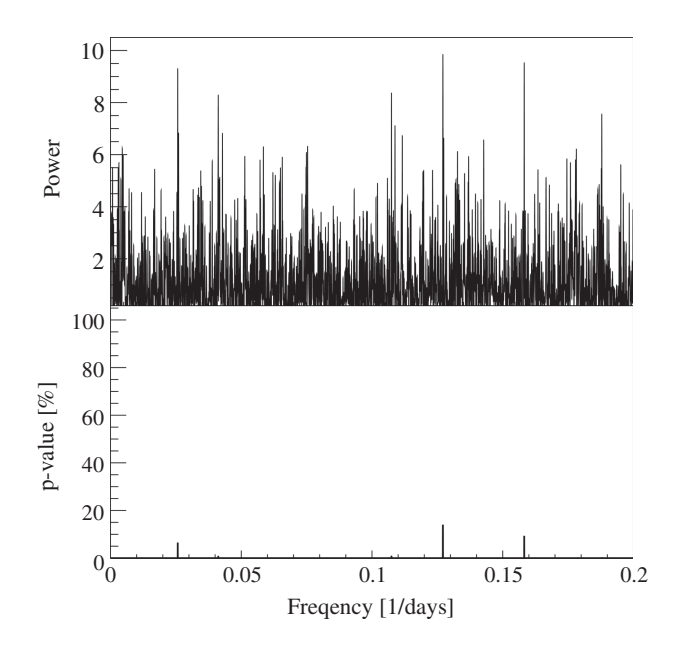


FIG. 2. Power distribution of likelihood method (top) and 1 - p (bottom) in percent for $1/R^2$ corrected five-day interval solar neutrino data, which is made by multiplying the original five-day interval data by the squared distance R^2 .

Figure 2 shows P_L values and (1-p) for the five-day sample. The maximum power is 9.9 at 0.126 days⁻¹ with (1-p) = 13.7%, which is the area of the distribution below a maximum power of 9.9. The results indicate no significant short-term periodic modulation in the measured SK solar neutrino data sample.

The sensitivity of the SK solar neutrino data to find a true periodicity is tested using a pseudoexperiment study. One thousand MC experiments are generated to simulate the five-day interval solar neutrino flux for each frequency (from $4 \times 10^{-4} \text{ days}^{-1}$ to 0.2 days⁻¹) and various modulation amplitudes. The power for each MC sample is calculated using a log-likelihood method. Figure 3 shows the sensitivity of finding the true period for given amplitudes and periods with 95% confidence level (CL). The false alarm criteria P_L is larger than 19.48 for a 98% chance of rejecting the null hypothesis. The sensitivity varies rapidly near 0.2 day⁻¹ close to the sampling frequency. For frequencies greater than 0.2 days⁻¹, amplitude fluctuation is canceled when the flux is averaged over a fiveday interval. The results indicate that the solar neutrino flux modulation is ruled out for amplitudes greater than 5.1% with 95% CL (or rule out greater than 5.2% amplitude with 90% CL for a 99% chance of rejecting the null hypothesis) in the frequency range of $< 0.15 \text{ days}^{-1}$. The results significantly improved compared to SK-I results (ruled out 10% amplitude) [16]. It is a factor 2 stronger constraint than the results from SNO (10.5% amplitude, 90% CL, and 99% false alarm) [18] as summarized in Table II.

Assuming the modulation of solar neutrino flux is only attributed to variations of the solar core temperature, as $\phi(\nu) = \alpha T^{25}$, where the α is a coefficient, the stability of the solar core temperature is $\delta T/T \simeq (1/25)\delta\phi(\nu)/\phi(\nu)$. Under this assumption, our result implies that the solar core

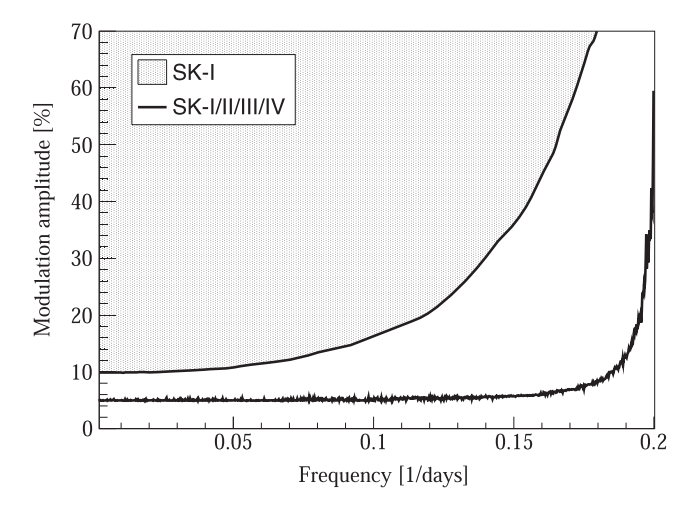


FIG. 3. The search sensitivity of solar neutrino modulation amplitude for each frequency with 95% CL. The shaded area is ruled out using SK-I solar neutrino data [16]. The solid curve shows the results of this analysis.

TABLE II. Comparison of time variation study results from SK, SNO, and Borexino experiments. The Kepler constants [eccentricity (ϵ) and perihelion shift ($\delta t_{\rm peri}$)] and sensitivity limit of amplitude (A_L) are from Refs. [18,19].

	€ [%]	$\delta t_{\rm peri}$ [days]	A_L [%] (CL)
SK (8B)	1.53 ± 0.35	-1.5 ± 13.5	5.2 (90%)
SNO (8B)	1.43 ± 0.86	-	10.5 (90%)
Borexino (⁷ Be)	1.84 ± 0.32	7 ± 20	-

temperature has less than 0.2% variations, which can be compared to the SK-I result of 0.4%.

The RSFP process and Mikheyev-Smirnov-Wolfenstein effect in a radiation zone or a tachocline of the Sun may cause potential modulations of solar neutrino flux. The probability of electron neutrino disappearance is numerically estimated with an exponent reduction factor for a magnetic field B and a magnetic moment μ ,

$$P_{\nu_e \to \nu_e} = \frac{1}{2} [1 - \cos 2\theta_v (1 - 2P(\mu B = 0)e^{-C\pi(\mu B)^2})],$$

where θ_v is the vacuum mixing angle, P is a hopping probability of mass eigenstates in the passage through the resonance region [20]. The C consists of the squared neutrino mass difference, neutrino energy, and a constant exponent proportional to the electron density [21]. For the large mixing angle solution, with an average solar magnetic field of 10^5 G and a neutrino's magnetic moment less than $10^{-11}~\mu_{\rm B}$, flux modulation is expected to be less than 2% [20,22], and the sole RSFP effect in solar amplitude is less than 0.1% [20]. These are yet to be probed in future experiments.

In the former study in Ref. [16], we searched for solar neutrino flux modulations using the Lomb-Scargle periodogram method [23,24]. We performed the period search using the same method to compare the results directly.

In the Lomb-Scargle method, the normalized Lomb power is given by

$$\begin{split} P_N(\omega) &\equiv \frac{1}{2\sigma^2} \left(\frac{[\Sigma_j(\phi_j - \bar{\phi})\cos\omega(t_j - \tau)]^2}{\Sigma_j \cos^2\omega(t_j - \tau)} \right. \\ &+ \frac{[\Sigma_j(\phi_j - \bar{\phi})\sin\omega(t_j - \tau)]^2}{\Sigma_j \sin^2\omega(t_j - \tau)} \right), \end{split}$$

where the measured flux in the jth bin is ϕ_j . The average time with live time weight in the jth bin is t_j , ω is the frequency for the test, $\bar{\phi} \equiv \sum_{i=1}^N \phi_i/N$, $\sigma^2 \equiv \sum_{i=1}^N (\phi_i - \bar{\phi})^2/(N-1)$, and offset time τ is defined by $\tan(2\omega\tau) \equiv (\sum_j \sin 2\omega t_j)/(\sum_j \cos 2\omega t_j)$. We scanned 100 000 frequencies in the range of 10^{-6} days⁻¹ to 0.2 days⁻¹. A maximum Lomb power of 9.39 is observed at the frequency 0.143 days⁻¹. To evaluate CL, 10 000 MC experiments are generated. Random Gaussian fluctuations at a measured

mean flux value and the measured standard deviations are used as the error values. The mean of gaussian is 2.36×10^6 cm⁻² s⁻¹ and the error is 0.486×10^6 cm⁻² s⁻¹. 34.3% of these MC experiments exceeding maximum power 9.39. Therefore, we found no significant periodic modulation in the five-day solar neutrino sample using the Lomb-Scargle method. We tested the generalized Lomb-Scargle method to consider the errors in each data point [25], and found no modulation either.

Annual modulation.—We test the annual variation of the solar neutrino flux, which changes by about 7% due to the Kepler orbital eccentricity of the Earth around the Sun. We divide the solar neutrino data into 12 bins for each SK run period. Each bin width corresponds to 365.25/12, and all years for the SK period are combined. For example, the first bin of SK-IV includes 10 months of statistics for a 10-year data taking. Figure 4 shows the distribution for each SK phase. To check consistency with astronomical data, we minimize a χ^2 for the solar neutrino flux at 1 A.U., the eccentricity ϵ and the perihelion shift $\delta t_{\rm peri}$ to the astronomically observed perihelion $t_{\rm peri}$:

$$\begin{split} \chi^2 &= \sum_{p} \biggl[\sum_{b=1}^{12} \biggl(\frac{D_{p,b} - E_{p,b}(f,\epsilon,\delta t_{\text{peri}},\delta_p)}{\sigma_{p,b}^{\text{stat.}}} \biggr)^2 + \delta_p^2 \biggr], \\ E_{p,b} &= \frac{f \bigl(1 - \delta_p \sigma_p^{\text{flux syst}} \bigr)}{r_b^2 \bigl(\epsilon, t_{\text{peri}} + \delta t_{\text{peri}} \bigr)}, \end{split}$$

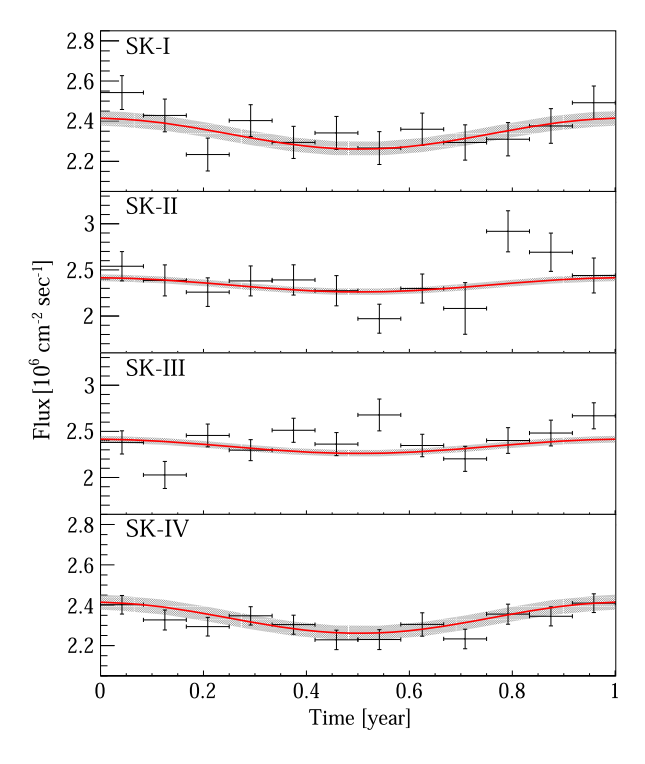


FIG. 4. The seasonal variation of the solar neutrino flux for SK-I/II/III/IV. The red curve and shade are flux and error in best fit, $f = (2.335 \pm 0.036) \times 10^6 \text{ cm}^{-2} \text{ s}^{-1}$ at 1 A.U. times inverse of squared distance between the Sun and the Earth.

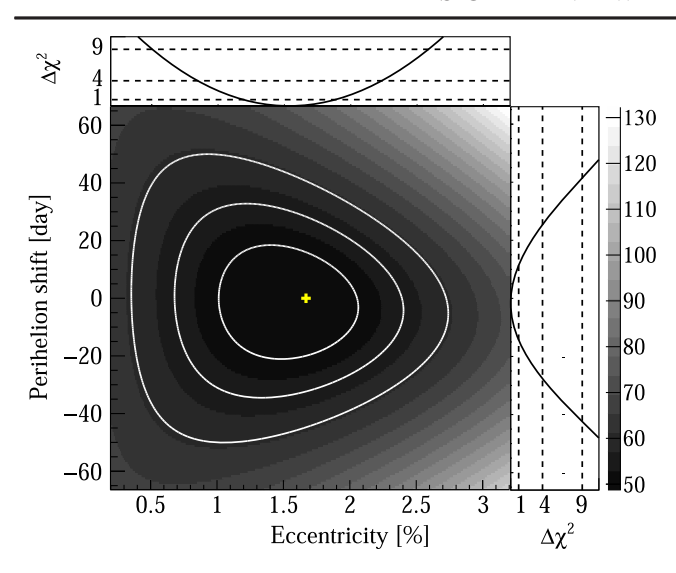


FIG. 5. $\Delta \chi^2$ for Kepler constants (ϵ, t_p) with contours $\Delta \chi^2 = 1\sigma, 2\sigma, 3\sigma; \quad \epsilon = (1.53 \pm 0.35)\%$ (expected value = 1.67%, yellow cross), $\delta t_{\rm peri} = (-1.5 \pm 13.5)$ days shifted from January 3 with minimum $\chi^2/{\rm NDF} = 48.74/(48-3)$.

where $D_{p,b}$ is total solar neutrino flux for each SK run $p=\mathrm{I}$, II, III, IV and month b=1–12. $E_{p,b}$ is the expected flux with statistical error $\sigma_{p,b}^{\mathrm{stat}}$. r_b is the distance from the Sun to the Earth, and f is the flux at 1 A.U. The total number of bins is 48 with three free parameters $(f, \epsilon, \delta t_{\mathrm{peri}})$, four nuisance parameters δ_p , and four systematic errors $\sigma_p^{\mathrm{flux \ syst}}$. The systematic errors are different because the SK detector is renovated for each period, such as installation of more photomultiplier tubes, change of data acquisition system, etc. [1–4]. The χ^2 minimization is carried out by scanning a 400×400 grid $(\epsilon, \delta t_{\mathrm{peri}})$ parameter space. Figure 5 shows the $\Delta \chi^2$ contour of eccentricity and perihelion parameters.

The best fit of eccentricity is $\epsilon = (1.53 \pm 0.35)\%$ which is consistent with the astronomical observation of 1.67%. The best fit of perihelion date shifted $\delta t_{\rm peri} = (-1.5 \pm$ 13.5) days from the expected date (January 3). The minimum χ^2/NDF (number of d.o.f.) is 48.74/(48-3). The measured average solar neutrino flux at 1 A.U. is $f = (2.335 \pm 0.036) \times 10^6 \text{ cm}^{-2} \text{ s}^{-1}$, where four nuisance parameters, δ_{LILIILIV} , for the best fit are -0.23, -0.16, -0.60, 0.62. The observed annual modulation of the solar ⁸B neutrino flux is consistent with a flux proportional to the inverse of the squared distance between the Sun and the Earth. This is consistent with the other results of solar neutrino experiments. Borexino experiment measures $\epsilon = (1.84 \pm 0.32)\%$, $\delta t_{\text{peri}} = (7 \pm 20)$ days from the seasonal flux of ⁷Be solar neutrino flux data [19]. The SNO experiment measures $\epsilon = (1.43 \pm 0.86)\%$ [18]. The results are summarized in Table II.

Conclusion.—We presented a time variation study of solar neutrino flux at Super-Kamiokande over 5804 days

(SK-I, II, III, IV). The flux of solar neutrinos exhibits annual modulation. The Kepler constants for the Earth-Sun orbit are evaluated. The measured eccentricity $(1.53 \pm 0.35)\%$ and perihelion shift (-1.5 ± 13.5) days are consistent with astronomical measurements. The potential periodic modulation is tested with five-day interval solar neutrino data using the likelihood and Lomb-Scargle periodogram methods. The results indicate that there is no significant solar neutrino flux modulation greater than 5.1% ($< 0.15 \text{ days}^{-1}$) of modulation amplitude.

We gratefully acknowledge the cooperation of the Kamioka Mining and Smelting Company. The Super-Kamiokande experiment has been built and operated from funding by the Japanese Ministry of Education, Culture, Sports, Science and Technology; the U.S. Department of Energy; and the U.S. National Science Foundation. Some of us have been supported by funds from the National Research Foundation of Korea (NRF-2009-0083526, NRF-2022R1A5A1030700, NRF-2022R1A3B1078756) funded by the Ministry of Science, Information and Communication Technology (ICT); the Institute for Basic Science (IBS-R016-Y2); and the Ministry of (2018R1D1A1B07049158, Education 2021R1I1A1 A01042256, 2021R1I1A1A01059559); the Japan Society for the Promotion of Science; the National Natural Science Foundation of China under Grants No. 12375100; the Spanish Ministry of Science, Universities and Innovation (Grant No. PID2021-124050NB-C31); the Natural Sciences and Engineering Research Council (NSERC) of Canada; the Scinet and Westgrid consortia of Compute Canada; the National Science Centre (UMO2018/30/E/ ST2/00441 and UMO-2022/46/E/ST2/00336) and the Ministry of Science and Higher Education (2023/WK/ 04), Poland; the Science and Technology Facilities Council (STFC) and Grid for Particle Physics (GridPP), UK; the European Union's Horizon 2020 Research and Innovation Programme under the Marie Sklodowska-Curie Grant Agreement No. 754496; H2020-MSCA-RISE-2018 JENNIFER2 Grant Agreement No. 822070, H2020-MSCA-RISE-2019 SK2HK Grant Agreement No. 872549; and European Union's Next Generation EU/PRTR Grant No. CA3/RSUE2021-00559; the National Institute for Nuclear Physics (INFN), Italy.

^{*}Also at BMCC/CUNY, Science Department, New York, New York 10007, USA.

Also at University of Victoria, Department of Physics and Astronomy, PO Box 1700 STN CSC, Victoria, British Columbia V8W 2Y2, Canada.

^[1] J. H. Hosaka *et al.*, Solar neutrino measurements in Super-Kamiokande-I, Phys. Rev. D **73**, 112001 (2006).

^[2] J. P. Cravens *et al.*, Solar neutrino measurements in Super-Kamiokande-II, Phys. Rev. D **78**, 032002 (2008).

- [3] K. A. Abe *et al.*, Solar neutrino measurements in Super-Kamiokande-III, Phys. Rev. D **83**, 052010 (2011).
- [4] K. A. Abe *et al.*, Solar neutrino measurements in Super-Kamiokande-IV, Phys. Rev. D **94**, 052010 (2016).
- [5] Q. R. Ahmad *et al.*, Direct evidence for neutrino flavor transformation from neutral-current interactions in the sudbury neutrino observatory, Phys. Rev. Lett. 89, 011301 (2002).
- [6] J. N. Bahcall, M. H. Pinsonneault, and S. Basu, Solar models: Current epoch and time dependences, neutrinos, and helioseismological properties, Astrophy. J. 555, 990 (2001).
- [7] J. N. Bahcall, S. Basu, and M. Pinsonneault, How uncertain are solar neutrino predictions?, Phys. Lett. B **433**, 1 (1998).
- [8] S. Turck-Chieze and I. Lopes, Toward a unified classical model of the Sun: On the sensitivity of neutrinos and helioseismology to the microscopic physics, Astrophys. J. 408, 347 (1993).
- [9] E. Akhmedov, Resonant amplification of neutrino spin rotation in matter and the solar-neutrino problem, Phys. Lett. B **213**, 64 (1988).
- [10] C. S. Lim and W. J. Marciano, Resonant spin-flavor precession of solar and supernova neutrinos, Phys. Rev. D 37, 1368 (1988).
- [11] J. Pulido, Predictions for the neutrino flavour mass squared difference and magnetic moment from solar neutrino observations, Phys. Lett. B 323, 36 (1994).
- [12] P. Sturrock, L. Bertello, E. Fischbach, D. Javorsek, J. Jenkins, A. Kosovichev, and A. Parkhomov, An analysis of apparent r-mode oscillations in solar activity, the solar diameter, the solar neutrino flux, and nuclear decay rates, with implications concerning the Sun's internal structure and rotation, and neutrino processes, Astropart. Phys. 42, 62 (2013).
- [13] S. Couvidat, R. A. García, S. Turck-Chièze, T. Corbard, C. J. Henney, and S. Jiménez-Reyes, The rotation of the deep solar layers, Astrophys. J. 597, L77 (2003).

- [14] S. Fukuda et al., The Super-Kamiokande detector, Nucl. Instrum. Methods Phys. Res., Sect. A 501, 418 (2003).
- [15] B. Aharmim *et al.*, Determination of the ν_e and total ⁸B solar neutrino fluxes with the Sudbury neutrino observatory phase I data set, Phys. Rev. C **75**, 045502 (2007).
- [16] J. Yoo et al., Search for periodic modulations of the solar neutrino flux in Super-Kamiokande-I, Phys. Rev. D 68, 092002 (2003).
- [17] See Supplemental Material at http://link.aps.org/ supplemental/10.1103/PhysRevLett.132.241803 for the data of this Letter.
- [18] B. Aharmim *et al.*, Search for periodicities in the ⁸B solar neutrino flux measured by the Sudbury Neutrino Observatory, Phys. Rev. D **72**, 052010 (2005).
- [19] S. Appel et al., Independent determination of the Earth's orbital parameters with solar neutrinos in Borexino, Astropart. Phys. 145, 102778 (2023).
- [20] A. B. Balantekin and C. Volpe, Does the neutrino magnetic moment have an impact on solar neutrino physics?, Phys. Rev. D **72**, 033008 (2005).
- [21] A. B. Balantekin and J. F. Beacom, Semiclassical treatment of matter-enhanced neutrino oscillations for an arbitrary density profile, Phys. Rev. D 54, 6323 (1996).
- [22] D. Caldwell and P. Sturrock, Evidence for solar neutrino flux variability and its implications, Astropart. Phys. 23, 543 (2005)
- [23] N. R. Lomb, Least-squares frequency analysis of unequally spaced data, Astrophys. Space Sci. 39, 447 (1976).
- [24] J. D. Scargle, Studies in astronomical time series analysis. II. Statistical aspects of spectral analysis of unevenly spaced data, Astrophys. J. 263, 835 (1982).
- [25] M. Zechmeister and M. Kürster, The generalised Lomb-Scargle periodogram: A new formalism for the floating-mean and Keplerian periodograms, Astron. Astrophys. 496, 577 (2009).